



Theoretical Investigation on Molecular Structure-Chemical Quantum Calculation of 7-Methyl-1,2,3-Triazole[4,5-c]Pyridine (DFT-Based *ab-initio* Technique)

Eslam Abo Alwafa ¹ and Abudelrhman Faraj ¹

¹Department of Chemistry, Faculty of Science, University of Sebha, Libya.

DOI: <https://doi.org/10.37375/sjfssu.v5i1.2914>

A B S T R A C T

ARTICLE INFO:

Received 27 August 2024.

Accepted 03 March 2025

Available 17 April 2025

Keywords:

7-methyl-1,2,3-triazole[4,5-c]pyridine, tautomerization, DFT, IR

Theoretical investigation of 1H- and 3H-7-methyl-1,2,3-triazole[4,5-c]pyridine tautomers and chemical quantum calculation have been studied using density function theory (DFT) (PED, optimized bond lengths and angles) at the B3LYP/6-31G(d,p) level.

The result reveals Optimized bond lengths and angles in good agreement with X-ray data of other triazole-pyridine compounds. The result of chemical quantum calculation reveals that the vibrational characteristics of the triazole compound display several distinct patterns that remain almost unchanged in the vibrations of compounds containing the same structure. The vibrational characteristics of the triazole-pyridine system show distinct patterns that are consistent across similar compounds with the same core structure.

The findings highlight the transferability of vibrational patterns in triazole-pyridine systems, which is useful for spectroscopic identification and further chemical design.

1 Introduction

Heterocyclic compounds are an integral part of organic chemistry, constituting more than 65% of organic chemistry (Pozharskii et al., 2011). They are cyclic organic compounds in which the ring contains at least one atom of an element other than carbon, and triazole-pyridine compounds constitute an essential part of these compounds used in various applications. Triazole compounds are characterized by their biological effects through their antibacterial, antifungal and antiparasitic effects (Karnaš et al., 2024; Marepu et al., 2018; Soumya et al., 2017). Therefore, they have been used in the manufacture of some medical antifungal drugs, such as fluconazole and isavuconazole, and in the manufacture of insecticides to protect plants from fungi, such as

paclobutrazol (Asif, 2015; Nagaraj et al., 2015; Tian et al., 2024).

The triazole ring connected to the pyridine ring in the studied compound is one of the essential electron-giving compounds. Due to its chemical composition and analysis of elements, it is also considered a material with a high nitrogen content (Bhatia & Dewangan, 2024; Zhao et al., 2023). They are used to prepare some drugs, such as tazobactam and mubritinib (da SM Forezi et al., 2018). In this paper, the Geometric optimization shape of the compound was calculated (Obtaining the best stable geometry for the compound) and the molecular spectra of the compound were studied theoretically by using density function theory (DFT).

DFT is a versatile tool within the ab initio framework that allows researchers to understand the electronic and chemical properties of molecules across a wide range of systems, making it applicable to various molecular systems and their properties (Butera, 2024; Madsen et al., 2021).

The main method for studying the molecular spectra of any compound, no matter how complex the structure, is infrared spectra, IR, which depends on the interaction of infrared radiation with the molecules, where the molecule absorbs this radiation and converts its energy into vibrational energy for the atoms that construct the molecule (Byrne et al., 2016). Each molecule has different vibrational patterns that depend on the number of atoms that make it up.

The main goal of the density functional theory is to replace the wave function with the density function with only three variables (x-position, y-position, and z-position of the electrons) and make it a base for calculation. Therefore, treating it as a mathematical or physical concept is much easier. The DFT principle is a reformulation of the quantum problem and its transformation from an issue of a multiparticle system to a single-particle matter (Zavatski et al., 2024). The theoretical DFT results are quite satisfactorily close to experimental data and relatively cheap with traditional methods that consume both money and time (Koch & Holthausen, 2015; Medvedev et al., 2017).

The results of chemical computing had an essential role in studying and solving complex and overlapping problems in the study of the system and seeing its results clearly, which simplified the determination of the structure of the studied system.

2 Chemical quantum calculation

The molecular structure of the studied compound was studied at the theoretical density function (DFT) level using the Lee-Yang-Parr correlation functional (B3LYP), the 6-31G(d,p) basis has been used (Miehlich et al., 1989).

IR wavenumbers as well as the band intensities were also calculated at the same DFT level using Gaussian 09W software (Frisch et al., 2009).

3 Results

The geometric parameters of the compound 1H & 3H-7MTP[4,5-c] (Fig. 1-2) were calculated and compared with the compound 1H&3H-7MTP[4-5-b] [6] (Fig. 3-4) (see Table 1).

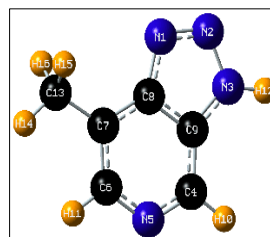


Fig. 1: 1H-7MTP[4,5-c]

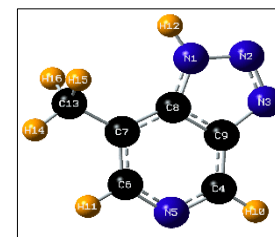


Fig. 2: 3H-7MTP[4,5-c]

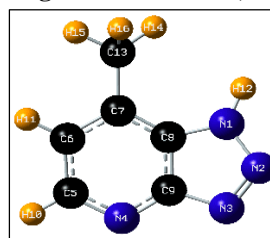


Fig. 3: 1H-7MTP[4,5-b]

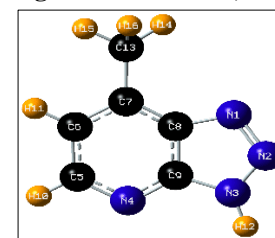


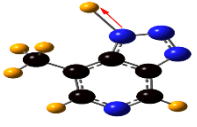
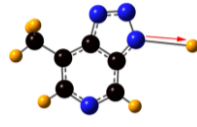
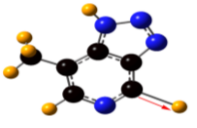
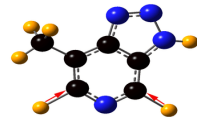
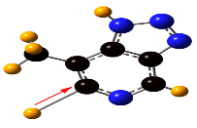
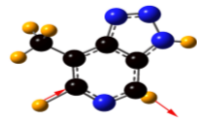
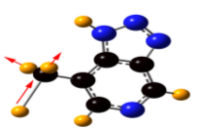
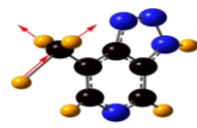
Fig. 4: 3H-7MTP[4,5-b]

Table 1: Calculated geometrical parameters of 7MTP(4,5-c) using DFT at B3LYP/6-31G(d,p) level, and comparison with 7MTP(4,5-b) (Lorenc et al., 2007) and experimental X-ray data for 7MTPHcNO₃.H₂O (Dymińska et al., 2017)

Bond length (Å°) and angles (°)	Optimized parameters from DFT data B3LYP/6-31G(d,p)				Experimental values (Dymińska et al., 2017)
	7MTP(4,5-c)		7MTP(4,5-b) (Lorenc et al., 2007)		
	1H	3H	1H	3H	
N1-N2/(N2-N3)	1.372 Å	1.362 Å	1.370 Å	1.363 Å	1.352 Å
N2=N3/(N1=N2)	1.288 Å	Å 1.293	1.289 Å	1.293 Å	1.292 Å
N1-C8/(N3-C9)	1.361 Å	Å 1.365	1.361 Å	1.363 Å	1.343 Å
N1-H12/(N3-H12)	1.008 Å	Å 1.009	1.008 Å	1.009 Å	--
N3-C9/(N1-C8)	1.382 Å	Å 1.380	1.383 Å	1.378 Å	1.381 Å
C4-N5*(N4-C5)	1.326 Å	Å 1.330	1.327 Å	1.334 Å	1.320 Å

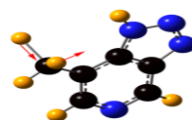
C6-C7	1.391 Å	Å 1.391	1.389 Å	1.392 Å	1.365 Å
C6-H11	1.088 Å	Å 1.087	1.086 Å	1.086 Å	--
C4-H10*(C5-H10)	1.087 Å	Å 1.087	1.088 Å	1.088 Å	--
C7-CH3	1.504 Å	Å 1.501	1.504 Å	1.501 Å	1.493 Å
C8-C9	1.406 Å	Å 1.406	1.411 Å	1.407 Å	1.392 Å
C7-C8	1.406 Å	Å 1.408	1.406 Å	1.408 Å	1.406 Å
C13-H14	1.092 Å	Å 1.092	1.092 Å	1.092 Å	--
C13-H15	1.096 Å	Å 1.095	1.096 Å	1.095 Å	--
C13-H16	1.096 Å	1.095 Å	1.096 Å	1.095 Å	--
N2=N3-C9/(N2=N1-C8)	108.5°	108.4°	108.4°	108.3°	107.5°
N1-N2-N3	108.7°	108.8°	109.0°	108.8°	109.8°
N2-N1-C8/(N2-N3-C9)	110.7°	110.7°	110.5°	110.7°	110.1°
C4-N5-C6*(C9-N4-C5)	118.9°	119.6°	114.0°	112.3°	123.9°

Table (2): vibrational normal modes of the 1H-7MTP and 3H-7MTP using DFT at the B3LYP/6-31G(d,p) level.

1H-7-methyl-1,2,3-triazole[4,5-c]pyridine	3H-7-methyl-1,2,3-triazole[4,5-c]pyridine
<p>v1=3677cm-1 100 -vNH</p> 	<p>v1=3673cm-1 100 - vNH</p> 
<p>v 2=3186 cm-1 99 - vCH</p> 	<p>v 2=3174 cm-1 100 - vCH</p> 
<p>v 3=3165cm-1 99 - vCH</p> 	<p>v 3=3170 cm-1 100- vCH</p> 
<p>v 4=3133cm-1 86 - vas (CH3)</p> 	<p>v 4=3136 cm-1 100 - vas (CH3)</p> 

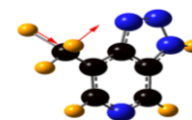
v 5=3086 cm-1

100 - vas (CH3)



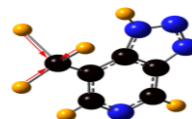
v 5=3110 cm-1

100 - vas (CH3)



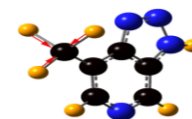
v 6=3034 cm-1

100 - vs (CH3)



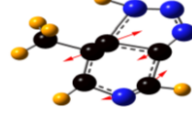
v 6=3051 cm-1

100 - vs (CH3)



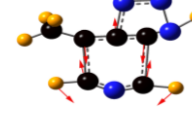
v 7=1663 cm⁻¹

57 - v Φ_P + 23-vΦ_T



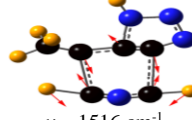
v 7=1647 cm⁻¹

48 - v Φ_P + 16-v Φ_T



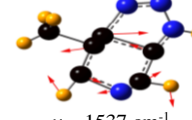
v 8=1635 cm⁻¹

69 - v Φ_P

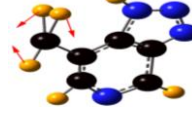


v 8=1639 cm⁻¹

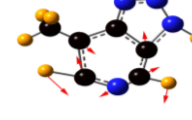
57 - v Φ_P



v 9=1516 cm⁻¹
13 - v Φ_P + 48 - δ_{as}(CH₃)

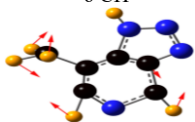


v 9=1537 cm⁻¹
35 - v Φ_P + 23 - δ CH + 12-δNH



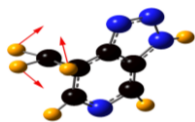
$$\nu_{10}=1513\text{ cm}^{-1}$$

$$28 - \nu \Phi_P + 20 - \delta_{as}(\text{CH}_3) + 18 - \delta \text{ CH}$$



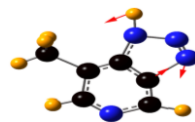
$$\nu_{10}=1508\text{ cm}^{-1}$$

$$72 - \delta_{as}(\text{CH}_3)$$



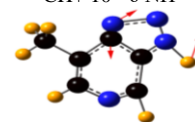
$$\nu_{19}=1273\text{ cm}^{-1}$$

$$37 - \nu \Phi_T + 15 - \delta \text{ CH}$$



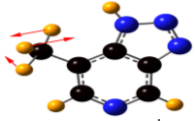
$$\nu_{19}=1249\text{ cm}^{-1}$$

$$50 - \nu \Phi_T + 12 - \nu \Phi_P + 13 - \delta \text{ CH} + 10 - \delta \text{ NH}$$



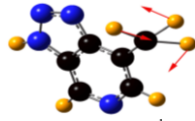
$$\nu_{11}=1498\text{ cm}^{-1}$$

$$93 - \delta_{as}(\text{CH}_3)$$



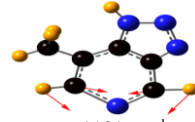
$$\nu_{11}=1491\text{ cm}^{-1}$$

$$92 - \delta_{as}(\text{CH}_3)$$



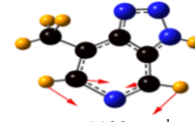
$$\nu_{20}=1165\text{ cm}^{-1}$$

$$65 - \nu \Phi_P + 12 - \delta \text{ CH}$$



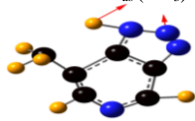
$$\nu_{20}=1170\text{ cm}^{-1}$$

$$45 - \nu \Phi_P$$



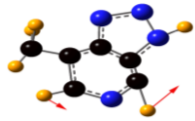
$$\nu_{12}=1458\text{ cm}^{-1}$$

$$24 - \nu \Phi_T + 20 - \nu \Phi_P + 15 - \delta \text{ NH} + 12 - \delta_{as}(\text{CH}_3)$$



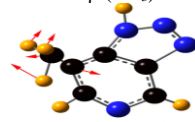
$$\nu_{12}=1459\text{ cm}^{-1}$$

$$13 - \nu \Phi_T + 26 - \delta \text{ CH} + 19 - \nu \Phi_P$$



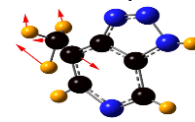
$$\nu_{21}=1101\text{ cm}^{-1}$$

$$42 - \nu (\text{C-CH}_3) + 17 - \nu \Phi_T + 13 - \rho (\text{CH}_3)$$



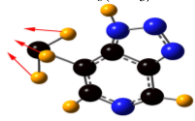
$$\nu_{21}=1122\text{ cm}^{-1}$$

$$30 - \nu (\text{C-CH}_3) + 15 - \delta \Phi_T + 10 - \nu \Phi_P$$



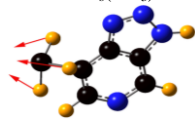
$$\nu_{13}=1434\text{ cm}^{-1}$$

$$68 - \delta_{as}(\text{CH}_3)$$



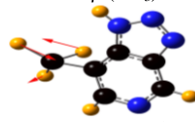
$$\nu_{13}=1431\text{ cm}^{-1}$$

$$92 - \delta_{as}(\text{CH}_3)$$



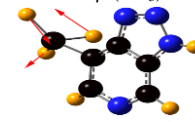
$$\nu_{22}=1067\text{ cm}^{-1}$$

$$80 - \rho (\text{CH}_3)$$



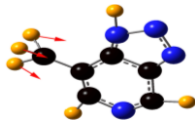
$$\nu_{22}=1066\text{ cm}^{-1}$$

$$78 - \rho (\text{CH}_3)$$



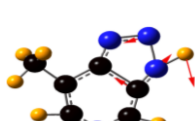
$$\nu_{14}=1429\text{ cm}^{-1}$$

$$68 - \delta_{as}(\text{CH}_3) + 19 - \delta \text{ CH} + 18 - \delta \text{ NH}$$



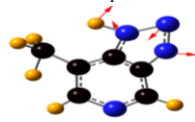
$$\nu_{14}=1413\text{ cm}^{-1}$$

$$21 - \delta \text{ NH} + 25 - \nu \Phi_T$$



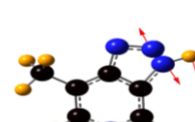
$$\nu_{23}=1010\text{ cm}^{-1}$$

$$52 - \nu \Phi_T + 18 - \rho (\text{CH}_3) + 15 - \nu \Phi_T$$



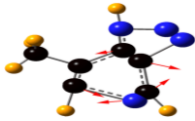
$$\nu_{23}=1030\text{ cm}^{-1}$$

$$86 - \nu \Phi_T$$



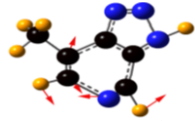
$$\nu_{15}=1391\text{ cm}^{-1}$$

$$21 - \nu \Phi_T + 50 - \nu \Phi_P$$



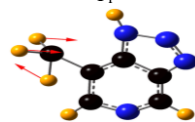
$$\nu_{15}=1372\text{ cm}^{-1}$$

$$53 - \nu \Phi_P + 11 - \nu \Phi_T$$



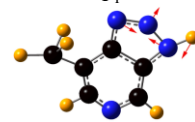
$$\nu_{24}=1001\text{ cm}^{-1}$$

$$35 - \rho (\text{CH}_3) + 23 - \delta \Phi_T + 11 - \nu \Phi_P$$



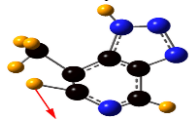
$$\nu_{24}=1012\text{ cm}^{-1}$$

$$48 - \delta \Phi_T + 25 - \rho (\text{CH}_3) + 15 - \nu \Phi_T$$



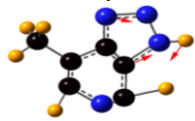
$$\nu_{16}=1345\text{ cm}^{-1}$$

$$27 - \delta \text{ CH} + 24 - \nu \Phi_T + 25 - \nu \Phi_P$$



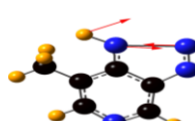
$$\nu_{16}=1344\text{ cm}^{-1}$$

$$27 - \delta \text{ CH} + 40 - \nu \Phi_T + 17 - \nu \Phi_P$$



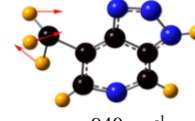
$$\nu_{25}=992\text{ cm}^{-1}$$

$$89 - \nu \Phi_T$$



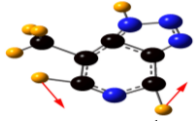
$$\nu_{25}=1001\text{ cm}^{-1}$$

$$31 - \rho (\text{CH}_3) + 24 - \delta \Phi_T + 11 - \nu \Phi_P$$



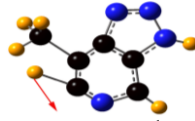
$$\nu_{17}=1308\text{ cm}^{-1}$$

$$39 - \delta \text{ CH} + 23 - \nu \Phi_T$$



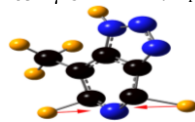
$$\nu_{17}=1323\text{ cm}^{-1}$$

$$44 - \delta \text{ CH} + 22 - \nu (\text{C-CH}_3)$$



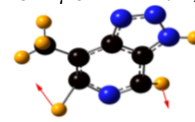
$$\nu_{26}=964\text{ cm}^{-1}$$

$$83 - \gamma \text{ CH} + 12 - \tau \Phi_P$$



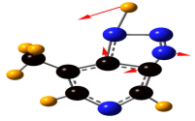
$$\nu_{26}=940\text{ cm}^{-1}$$

$$84 - \gamma \text{ CH} + 11 - \tau \Phi_P$$



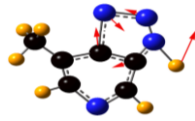
$$\nu_{18}=1291\text{ cm}^{-1}$$

$$28 - \delta \text{ NH} + 18 - \delta \Phi_T + 39 - \nu \Phi_T$$



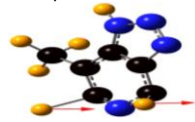
$$\nu_{18}=1291\text{ cm}^{-1}$$

$$41 - \nu \Phi_T + 16 - \delta \text{ NH} + 19 - \nu \Phi_P$$



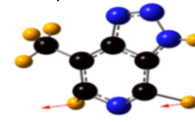
$$\nu_{27}=913\text{ cm}^{-1}$$

$$83 - \gamma \text{ CH} + 27 - \tau \Phi_P$$



$$\nu_{27}=886\text{ cm}^{-1}$$

$$75 - \gamma \text{ CH} + 39 - \tau \Phi_P$$



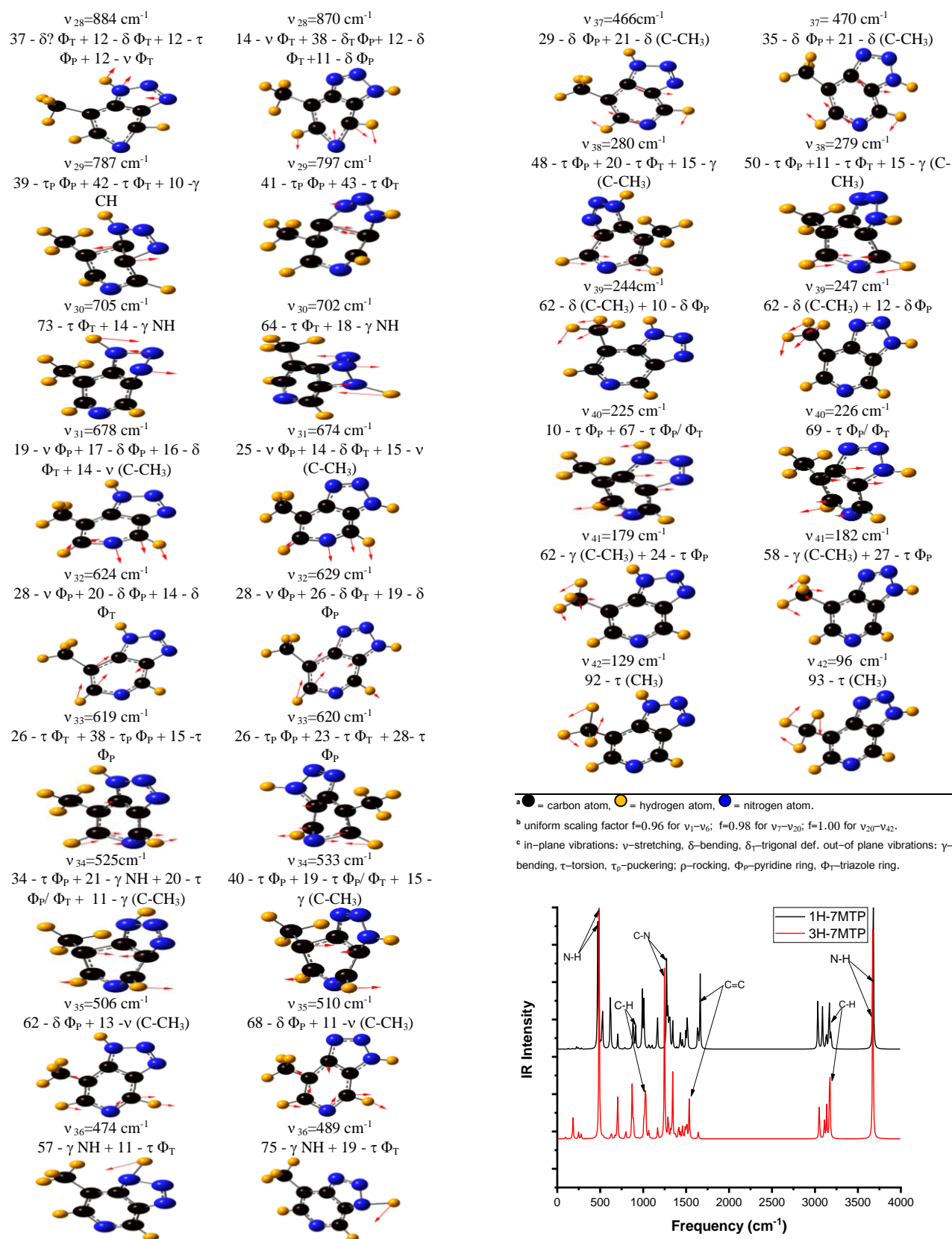


Fig.5:Theoretical infrared spectra of 1H,3H-7MTP isomers

4 Discussion

The geometric structure of 7MTP has been studied in several previous studies, and the double-ring system is the main component of this compound.

The results of the experimental geometric parameters (bond, lengths, and angles) of 7MTPHcNO₃.H₂O [14] and the geometric parameters of the compound 1H&3H-7MTP[4,5-b] (Fig. 3-4) [6] were taken to compare them with the theoretical results calculated for the two isomers 1H&3H-7MTP(4,5-c) (Fig. 1-2) using the theoretical density function DFT at the level B3LYP/6-31G(d, p) as in Table (1). The experimental and theoretical data agree very well that the 7MTP skeleton is planar; a discrepancy appears between the theoretical and experimental data of the C-H bond in the pyridine ring because the average length of the theoretical bond is 1.088 Å while the experimental one is .093 Å. In contrast, the rest of the engineering parameters for all bonds are close to each other, indicating that the B3LYP function is suitable for predicting the geometry of the studied compound.

The 7-MTP(4,5-c) has the formula C₆H₆N₄, and according to the law (3N) for calculating the vibrational, translational, and rotational movements, it has 48 movements, both for the 1H and 3H-tautomer. There were three translational movements, three rotational movements, and 42 vibrational movements (Carmer, 2002). These vibrations include 29 in-plane movements, 11 out-of-plane movements, and two movements are a mixture of in-plane and out-of-plane (Clark, 1985).

• In-plane movements

There are three vibrational movements in the plane; ν -stretching, δ -bending, and δ_T -trigonal def (see Table 2).

There are two types of Stretching and bending: symmetric (s) and asymmetric (as).

Symmetric stretching appears in: (ν -NH) at ν_1 by 100%, (ν -CH) at ν_2 , ν_3 by 99%, 100% for the 1H-3H-isomers, (ν -CH₃) at ν_6 by 100%, the pyridine ring (ν - Φ P) at ν_8 by 69%, and the rest of the pyridine ring symmetric stretching appear as a mixture of vibrations for the 1H-isomers at ν_7 , ν_9 , ν_{10} , ν_{12} , ν_{15} , ν_{16} , ν_{20} , ν_{24} , ν_{31} , ν_{32} , and for the 3H-isomers, they appear at ν_8 by 57%, while the rest of the stretching appear as mixtures at ν_7 , ν_9 , ν_{12} , ν_{15} , ν_{16} , ν_{18} , ν_{19} , ν_{20} , ν_{21} , ν_{25} , ν_{31} , ν_{32} (Dronskowski, 2008), and the

triazole ring (ν - Φ T) at ν_7 , ν_{12} , ν_{15} , ν_{16} , ν_{17} , ν_{18} , ν_{19} , ν_{21} , ν_{23} , ν_{25} , ν_{28} for 1H- isomers, and for 3H- isomers at ν_7 , ν_{12} , ν_{14} , ν_{15} , ν_{16} , ν_{18} , ν_{19} , ν_{23} , ν_{24} , ν_{28} (Schmidt et al., 2022).

Asymmetric stretching appears in: (ν as - CH₃) at ν_4 , ν_5 .

Symmetric bending appears in: (δ s-CH₃) at ν_{13} by 68%, 92% for the 1H, 3H- isomers, and at ν_{14} for the 1H-isomers, the pyridine ring (δ - Φ P) at ν_{31} , ν_{32} , ν_{35} , ν_{37} , ν_{39} for the isomers -1H and at ν_{28} , ν_{32} , ν_{35} , ν_{37} , ν_{39} for the -3H isomers, and triazole ring (δ - Φ T) at ν_{24} , ν_{28} , ν_{31} , ν_{32} for the 1H- isomers and at ν_{21} , ν_{24} , ν_{25} , ν_{28} , ν_{31} , ν_{32} for the 3H- isomers.

Symmetric bending appears in: (δ as-CH₃) at ν_{11} by 93%, 92% for the 1H, 3H- isomers, and the rest of the vibrations appear as a mixture at ν_9 , ν_{10} , ν_{12} for the 1H-isomers, and at ν_{10} for the 3H-isomers.

The trigonal def (δ_T) appears in: the pyridine ring (δ_T - Φ P) at ν_{18} for the 1H- isomers and at ν_{28} for the 3H-isomers (Dronskowski, 2008; Serdaroglu & Şahin, 2019).

• Out-of-plane movements

There are three types of vibrational movements out-of-plane; γ -bending, τ -torsion, and τ_p -puckering.

The bending appears in: (γ -CH) at ν_{26} , ν_{27} , ν_{29} for the 1H-isomers, and at ν_{26} , ν_{27} for 3H-isomers, (γ - NH) at ν_{30} , ν_{34} , ν_{36} for 1H isomers, and at ν_{30} , ν_{36} for 3H-isomer.

The twisting appears in; (τ -CH₃) at ν_{42} by 92% for the 1H- isomers, and at ν_{42} by 93% for the 3H- isomers, the pyridine ring (τ - Φ P) at ν_{26} , ν_{28} , ν_{33} , ν_{34} , ν_{38} , ν_{40} , ν_{41} for the 1H-isomers and at ν_{26} , ν_{33} , ν_{34} , ν_{38} , ν_{41} for the 3H-isomers, the triazole ring (τ - Φ T) at ν_{29} , ν_{30} , ν_{33} , ν_{36} , ν_{38} for the 1H, 3H-isomers.

Twisting of the pyridine ring and triazole ring together (τ - Φ P/ Φ T) appears at ν_{34} , and ν_{40} for the -1H and -3H isomers.

The puckering appears in: the pyridine ring (τ_p - Φ P) at ν_{27} , ν_{29} , and ν_{33} for the 1H, 3H-isomers.

• Mixture of in-plane and out-of-plane movements

The rocking movement (ρ) is a mixture of vibrational motions between in-plane and out-of-plane; it appears in the (ρ -CH₃) at ν_{22} by 80%, 78%

for the 1H, 3H-isomers, and it appear as mixtures at ν_{21} , ν_{23} , ν_{24} for the 1H-isomers, and at ν_{24} , ν_{25} for the 3H-isomers (Schmidt et al., 2022).

Theoretical infrared spectra of 1H, and 3H-isomers show in (Fig. 5).

Conflict of interest:

I declare that there are no conflicts of interest.

References

- Asif, M. J. C. I. (2015). Anti-neuropathic and anticonvulsant activities of various substituted triazoles analogues. *1*(4), 174-183.
- Bhatia, A. K., & Dewangan, S. (2024). N-Heterocyclics as Corrosion Inhibitors: Miscellaneous. In *Handbook of Heterocyclic Corrosion Inhibitors* (pp. 249-270). CRC Press.
- Butera, V. J. P. C. C. P. (2024). Density functional theory methods applied to homogeneous and heterogeneous catalysis: a short review and a practical user guide.
- Byrne, H. J., Knief, P., Keating, M. E., & Bonnier, F. J. C. S. R. (2016). Spectral pre and post processing for infrared and Raman spectroscopy of biological tissues and cells. *45*(7), 1865-1878.
- Carmer, C. J. (2002). Essential of Computational Chemistry. In: Chichester: John Wiley and Sons, Ltd.
- Clark, T. (1985). A Handbook of Computational Chemistry-J. Wiley and Sons, New York.
- da SM Forezi, L., Cardoso, M. F., Gonzaga, D. T., de C da Silva, F., & Ferreira, V. F. J. C. T. i. M. C. (2018). Alternative routes to the click method for the synthesis of 1, 2, 3-triazoles, an important heterocycle in medicinal chemistry. *18*(17), 1428-1453.
- Dronskowski, R. (2008). *Computational chemistry of solid state materials: a guide for materials scientists, chemists, physicists and others*. John Wiley & Sons.
- Dymińska, L., Sheweshen, K. S. M., Gağor, A., Lorenc, J., & Hanuza, J. J. J. o. M. S. (2017). Crystal and molecular structures, IR and Raman spectra, vibrational dynamics of aquo 7-methyl-1H-[1, 2, 3] triazolo [4, 5-c] pyridinium nitrate—a new composite material. *1133*, 9-17.
- Frisch, M., Trucks, G., Schlegel, H., Scuseria, G., Robb, M., Cheeseman, J., . . . Petersson, G. J. G. I. (2009). Gaussian 09, Revision B. 01 (Wallingford, CT).
- Karnaš, M., Rastija, V., Vrandečić, K., Čosić, J., Kanižai Šarić, G., Agić, D., . . . Molnar, M. J. J. o. T. U. f. S. (2024). Synthesis, antifungal, antibacterial activity, and computational evaluations of some novel coumarin-1, 2, 4-triazole hybrid compounds. *18*(1), 2331456.
- Koch, W., & Holthausen, M. C. (2015). *A chemist's guide to density functional theory*. John Wiley & Sons.
- Lorenc, J., Dymińska, L., Mohmed, A. F., Hanuza, J., Talik, Z., Maćzka, M., & Macalik, L. J. C. p. (2007). Vibrational dynamics and molecular structure of 1H- and 3H-1, 2, 3-triazolo [4, 5-b] pyridine and its methyl-derivatives based on DFT chemical quantum calculations. *334*(1-3), 90-108.
- Madsen, J., Pennycook, T. J., & Susi, T. J. U. (2021). ab initio description of bonding for transmission electron microscopy. *231*, 113253.
- Marepu, N., Yeturu, S., Pal, M. J. B., & letters, m. c. (2018). 1, 2, 3-Triazole fused with pyridine/pyrimidine as new template for antimicrobial agents: Regioselective synthesis and identification of potent N-heteroarenes. *28*(20), 3302-3306.
- Medvedev, M. G., Bushmarinov, I. S., Sun, J., Perdew, J. P., & Lyssenko, K. A. J. S. (2017). Density functional theory is straying from the path toward the exact functional. *355*(6320), 49-52.
- Miehlich, B., Savin, A., Stoll, H., & Preuss, H. J. C. P. L. (1989). Results obtained with the correlation energy density functionals of Becke and Lee, Yang and Parr. *157*(3), 200-206.
- Nagaraj, A., Sunitha, M., Sanjeeva, R. L., Vani, D. M., & Ch, S. R. J. O. C. (2015). Synthesis and biological evaluation of 3-benzyl/piperazino-methyl-1, 2, 3-triazol-4-yl)-2, 3-dihydro-1, 3, 4-thiadiazole-2-thione. *8*(3), 70.
- Pozharskii, A. F., Soldatenkov, A. T., & Katritzky, A. R. (2011). *Heterocycles in life and society: An introduction to heterocyclic chemistry, biochemistry and applications*. John Wiley & Sons.
- Schmidt, M., Abdul Latif, A., Prager, A., Gläser, R., & Schulze, A. J. F. i. c. (2022). Highly efficient one-step protein immobilization on polymer membranes supported by response surface methodology. *9*, 804698.
- Serdaroğlu, G., & Şahin, N. J. J. o. M. S. (2019). The synthesis and characterization of 1-(Allyl)-3-(2-methylbenzyl) benzimidazolium chloride: FT-IR, NMR, and DFT computational investigation. *1178*, 212-221.
- Soumya, T., Ajmal, C. M., Bahulayan, D. J. B., & Letters, M. C. (2017). Synthesis of bioactive and fluorescent pyridine-triazole-coumarin peptidomimetics through sequential click-multicomponent reactions. *27*(3), 450-455.
- Tian, Y., Song, Y., Qiao, Y., Song, L., Zhao, Q., Yin, D., . . . Therapeutics. (2024). Effects of Triazole Antifungal Agents on the Plasma Concentration and Dosage of Cyclosporin in Patients with Aplastic Anaemia. *2024*(1), 6850289.
- Zavatski, S., Neilande, E., Bandarenka, H., Popov, A., Piskunov, S., & Bocharov, D. J. N. (2024). Density functional theory for doped TiO₂: Current research strategies and advancements. *35*(19), 192001.
- Zhao, W., Zheng, X. D., Tang, P. Y. Z., Li, H. M., Liu, X., Zhong, J. J., & Tang, Y. J. J. M. R. R. (2023). Advances of antitumor drug discovery in traditional Chinese medicine and natural active products by using multi-active components combination. *43*(5), 1778-1808.